

ANALYSIS OF MELT WATER FREEZING  
IN THE ICE BOREHOLE

Fucheng Li



Polar Ice Coring Office  
University of Alaska Fairbanks  
Fairbanks, AK 99775-1710, USA

PICO  
TR-93-2

July 1993

## TABLE OF CONTENTS

	Page
LIST OF FIGURES .....	iii
ACKNOWLEDGMENTS .....	iv
ABSTRACT .....	v
SECTION 1. INTRODUCTION .....	1
SECTION 2. TEMPERATURE CHANGE OF A DESCENDING DRILL INTO AN ICE BOREHOLE .....	3
2.1 Standard Conditions .....	3
2.2 Drill Temperature Change as the Drill Descends in the Upper Borehole .....	5
2.3 Drill Temperature Change as the Drill Descends in the Lower Borehole .....	7
SECTION 3. FREEZING OF MELT WATER .....	11
3.1 Finite Element Formulation .....	11
3.2 Model Text .....	15
3.3 Standard Computation .....	16
3.4 Freezing of Slush .....	19
SECTION 4. CONCLUSIONS AND SUGGESTIONS .....	21
REFERENCES .....	23

## LIST OF FIGURES

	Page
Figure 1. Standard ice drill radius .....	3
Figure 2. Liquid temperature profile .....	4
Figure 3. Thin pipe radius .....	5
Figure 4. Sketch of drill temperature change as the drill descends .....	9
Figure 5. Three node isoparametric element .....	13
Figure 6. Temperature distribution in partially frozen water .....	15
Figure 7. Comparisons of phase locations vs. times .....	16
Figure 8. Standard modeling domain .....	17
Figure 9. Melt water freezing time vs. the phase locations .....	18
Figure 10. Freezing-up time of slush vs. percentage of ice chips .....	20

## ACKNOWLEDGMENTS

The author would like to express his sincere appreciation to Dr. John Kelley, Director of the Polar Ice Coring Office, and to Mr. Kerry Stanford, P. E., Manager of the Engineering Division, Polar Ice Coring Office, for their support and encouragement on this study. Also, thanks are extended to other staff members of the Polar Ice Coring Office, University of Alaska Fairbanks, for their kind assistance.

The research described herein was funded by the U. S. National Science Foundation and the University of Alaska Fairbanks through the Polar Ice Coring Office. The project funding was greatly appreciated.

## ABSTRACT

The remote sites and difficult environment cause ice drilling in cold, deep ice to be very time consuming and costly. One of the potential threats to the drill is freezing in the bottom of an ice borehole due to melt water. Two basic problems to be solved in studying the rate of melt water freezing are: 1) What is the drill temperature change as it is lowered into the borehole? and 2) How does the melt water freeze around the drill?

The heat exchange between the drill and the surrounding drill fluid is dominated by convection as the drill descends in the borehole. An analytical solution of the drill temperature change during descent was obtained by assuming the temperature varies only with time because the drill pipes (stainless steel) are very thin and have relatively high thermal conductivity. In the upper length of a borehole, it would take two minutes for the drill to change temperature by 20°C. During descent in the lower part of the borehole, the drill has a temperature lag behind that of the surrounding drill fluid, but only by a very small amount. For a descent speed of 0.53 m/s, the drill temperature change can be assumed to be the same as the surrounding fluid.

The melt water freezing around the drill in the bottom of a borehole is an axisymmetric, multiple phase-change problem. A finite element model has been developed to handle this special problem. An isoparametric element was used. The latent heat effects were taken into account through a Dirac delta function in the heat capacity. The Crank-Nicolson method ( $\theta = 0.5$ ) was used in the transient process modeling. Modeling results show that the freezing fronts close up first in the space between the outer pipe and the ice wall. For ice temperature of -5°C, it would take 75 minutes to freeze up. Freezing of slush with a different percentage (in volume) of ice chips in the melt water was also modeled. The results show that the freezing-up time was reduced 0.44 times, from 75 minutes for pure water to 35 minutes for 75%

ice chips in the water, at ice temperature of  $-5^{\circ}\text{C}$ . One may reduce the possibility of the drill freezing in the bottom of a borehole by slowly lowering the drill to the bottom of the borehole and/or moving the drill up and down when it reaches the bottom of a borehole.

## SECTION 1

### INTRODUCTION

For scientific research purposes, many ice-core drilling activities in deep, cold ice have been developed in Greenland and Antarctica, e.g., the ongoing project GISP-2 in Greenland where the ice drill is attempting to reach bedrock through more than 3000 m of ice sheet. The remote sites and difficult drilling environment make such drilling very time and cost consuming. Therefore, the drill performance is a critical consideration in the operation planning. Unfortunately, though polar-ice drilling is a unique challenge, there are still some problems with drilling to be investigated. One of the potential threats to the ice drill operation is the ice drill freezing into the bottom of the ice borehole through contact with melt water.

Because of the earth heat flux into the ice sheet from the bedrock, the bottom ice of an ice sheet is warm and may even be melted. Thus, there might be a layer of melt water between the ice sheet and the bedrock at a temperature near the freezing point of water. When the ice drill reaches the bedrock, the melt water may go up in the borehole around the drill due to pressure difference between the melt water and the drill fluid in the borehole. Due to the vertical temperature gradient in the ice sheet, which is greater in the bottom than in the upper part, there will be a temperature difference between the melt water and the ice borehole wall as well as the drill. Thus, the heat flow from the melt water to the drill and borehole wall produces freezing of melt water at the surfaces of the drill and the borehole wall. The space between the drill and the borehole wall is very small (less than 10 mm); therefore, the water might freeze within this small space a short time before the drill can be raised. In this case, the drill may become stuck at the bottom of the borehole.

From the point of view of the drill operator, the question is how long would one have to retrieve the drill from the bottom to prevent the drill being stuck by freezing? Or, in other words, how long would it take for the melt water to freeze the drill in the

borehole? There are two basic problems to be studied to answer this question. One is what the drill temperature is when it reaches the bottom of the borehole, or how the drill temperature changes as the drill is lowered in the borehole from the surface of the ice sheet. The other question is how fast the melt water freezes on the ice borehole wall and the drill surfaces under different conditions.

This report describes the methods used to solve these problems and the relative results. To solve the first problem, a simple analytical method was used. For the second problem, it is obvious that accurate modeling of heat transfer and freezing in the borehole is necessary. It is true that there are many general-purpose finite element programs available for thermal modeling. However, using a large general-purpose program to solve a specialized problem is often far more costly than to write a program expressly for solving the specialized problem. Also, two problems, the radial heat flow from melt water to both ice borehole wall and drill, and the multi-phase change of melt water at both the borehole wall and the drill surfaces, require development of a computer program and more detailed calculations. In this study, a finite element model was developed which can handle heat transfer problems in one-dimensional or axisymmetric coordinates and allow multiple phases in the model domain.



SECTION 2  
TEMPERATURE CHANGE OF A DESCENDING ICE DRILL  
INTO AN ICE BOREHOLE

The temperature of the ice drill is a dominant factor in water freezing on the drill surfaces. Therefore, one first has to estimate the temperature changes of an ice drill as it descends in the ice borehole.

2.1 Standard Conditions

The lower end of a standard drill used in the GISP-2 project in Greenland is made of two stainless steel, thin-walled pipes as the core barrel (Fig. 1). The internal pipe has an inner radius of 70 mm and an outer radius of 73.18 mm. The wall thickness is 3.18 mm. For the outer pipe, the inner and outer radii are 81.75 mm and 84.29 mm, respectively, with wall thickness of 2.54 mm. The drill is 25.5 m in length and weighs about 1300 pounds.

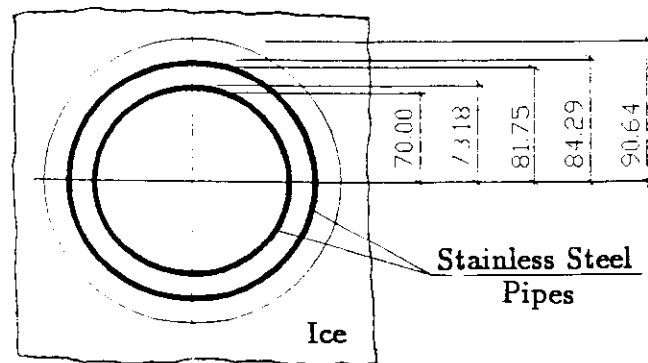


Figure 1. Standard ice drill radius for GISP-2 project in Greenland. Unit: mm.

The designed ice borehole is 90.64 mm in radius and 3200 m in depth. It is filled with n-butyl acetate liquid. This liquid temperature profile in the ice borehole can

be considered the same as the ice temperature profile shown in Figure 2. For model generation purposes, it is assumed that the borehole bottom temperature should be at the ice pressure melt point in order to have a melt-water layer, which may be calculated by  $-0.74^{\circ}\text{C}/1000\text{ m} \times 3200\text{ m} = -2.368^{\circ}\text{C}$  according to Spring (1981). It takes about 100 minutes to lower the drill to the bottom of the ice borehole from the ice surface, i.e., the average descent speed is 0.53 m/s.

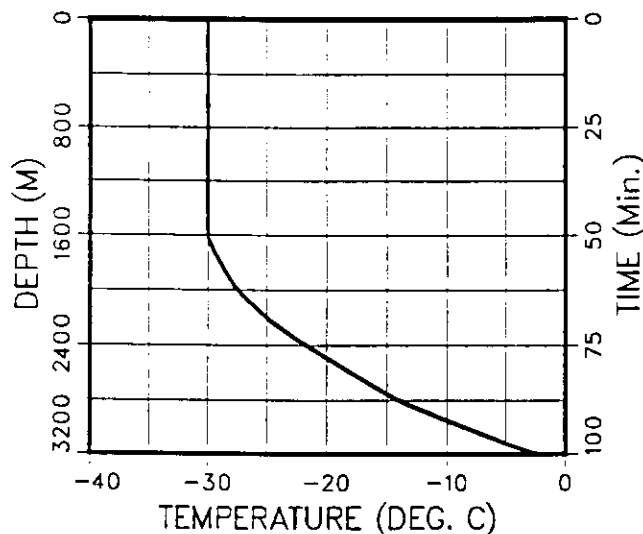


Figure 2. The liquid temperature profile in an ice borehole is assumed to be the same as the ice temperature profile. At the right edge is a time coordinate converted by time  $t = Z/V$ ,  $Z$  is depth and  $V$  is drill descent speed,  $V = 0.53\text{ m/s}$ .

Features of this assumed case are, from the point of view of heat transfer: 1) A radial heat flow is expected to be predominant in the heat transfer process; therefore, it can be treated as an axisymmetric problem; 2) When the drill descends in the borehole liquid, the relative motion of drill to liquid is similar to a pipe flow; therefore, the heat exchange at the drill surface is mainly controlled by convection of

the liquid at the surface; and 3) The pipe is very thin and has a relatively high thermal conductivity ( $K_s = 16.3 \text{ w/m}^\circ\text{C}$  for stainless steel).

## 2.2 Drill Temperature Change as the Drill Descends in the Upper Borehole

Consider a long, thin stainless pipe with inner radius of  $a$  and outer radius of  $b$  (Fig. 3). Because of its relatively high thermal conductivity and small thickness, the pipe temperature was assumed uniform in space and, therefore, varies only with time. At time zero it is placed and then moved in a fluid of a constant temperature.

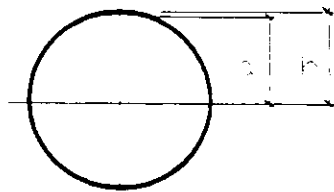


Figure 3. A thin stainless pipe with inner radius  $a$  and outer radius  $b$ .

A heat balance on the pipe, equating the time rate of change in heat capacity with convective heat loss, yields (Eckert and Drake, 1972)

$$C_v V \frac{dT}{dt} = -hA(T - T_f) \quad (2.1)$$

where

$C_v$  = the volume heat capacity

$V$  = the pipe volume

$T$  = the pipe temperature

$t$  = time

$h$  = heat convective coefficient

$A$  = the pipe inner and outer surface area

$T_f$  = the fluid emperature.

The initial condition is  $T = T_0$  at  $t = 0$ . Let

$$\theta = T - T_f \quad (2.2)$$

then equation (2.1) can be rewritten as

$$C_v \frac{d\theta}{dt} = -hA\theta \quad (2.3)$$

or

$$\frac{d\theta}{\theta} = -\frac{hA}{C_v} dt \quad (2.4)$$

and

$$\theta = \theta_0 = T_0 - T_f \text{ at } t = 0 \quad (2.5)$$

The solution to equations (2.4) and (2.5) is

$$\frac{\theta}{\theta_0} = e^{-\left(\frac{h}{C_v L}\right)t} \quad (2.6)$$

where  $L$  is the characteristic length,  $L = V/A$ . Further, equation (2.6) can be written as

$$t = -\frac{C_v L}{h} \ln\left(\frac{\theta}{\theta_0}\right) \quad (2.7)$$

or

$$t = -\frac{C_v L}{h} \ln\left(\frac{\Delta T}{\Delta T_0}\right) \quad (2.8)$$

where  $\Delta T = \theta = T - T_f$ , is the temperature difference of pipe to fluid,  $\Delta T_0$  is the initial temperature difference of pipe to fluid.

The parameters for a stainless pipe are: wall thickness of 2.54 mm,  $C_v = 3.67 \times 10^6 \text{ J/m}^3\text{C}$ , and

$$L = \frac{V}{A} = \frac{\pi(b^2 - a^2)}{2\pi b + 2\pi a} = \frac{b-a}{2} = 1.27 \times 10^{-3} \text{ m.}$$

The heat convective coefficient is dependent on fluid type. If the Reynolds number is greater than about 2000, the smooth pipe flow will generally be turbulent according to Kay (1963). The Reynolds number may be expressed as

$$Re = \frac{\rho U D}{\mu} \quad (2.9)$$

where  $\rho$  is the fluid density,  $U$  is the smooth relative speed,  $D$  is the pipe diameter, and  $\mu$  is the dynamic viscosity. For a stainless drill moving in an Acetate fluid at a speed of  $U = 0.5 \text{ m/s}$ , taking  $D = 0.17 \text{ m}$ ,  $\rho = 920 \text{ kg/cm}^3$  and  $\mu = 2 \times 10^{-3} \text{ N.s/m}^2$ , then  $Re = 39.1 \times 10^3$ . So a turbulent flow is expected around the drill. The heat convective coefficient for organic liquid has a range of  $h = 284 - 2840 \text{ w/m}^2 \text{ }^\circ\text{C}$  (Kay, 1963). A low value of  $h$  introduces a longer time for the pipe to change by the same temperature difference. To be conservative for practical cases, a low value of  $h = 284 \text{ w/m}^2\text{ }^\circ\text{C}$  was used here to calculate the time. For  $\Delta T/\Delta T_0 = 10^{-3}$ ,  $t = 113\text{-s} \approx 2 \text{ - min}$ . This means, after two minutes the drill temperature will differ from that of the Acetate liquid by only  $10^{-3}$  times the initial temperature difference. If the initial temperature difference is  $20^\circ\text{C}$ , then after two minutes, this difference will drop to  $0.02^\circ\text{C}$ . If this relatively small difference is neglected, then one can say that the drill temperature is the same as that of the Acetate liquid after it has been immersed in the upper borehole for two minutes.

### 2.3 Drill Temperature Change as the Drill Descends in the Lower Borehole

As shown in Figure 2, the Acetate liquid in the lower borehole has a temperature change, and the temperature gradient increases with depth. When descending to this part of the borehole, the drill encounters a fluid of varying temperature. This is similar to a pipe flow with varying flow temperature. Suppose the drill descent speed is a constant  $V$ ; the fluid temperature changing as depth  $Z$  can be converted to a temperature change with time by time  $t = Z/V$ , as shown in Figure 2

(time coordinate at the right edge). Suppose the fluid temperature  $T_f$  changes linearly with local depth as

$$T_f = a + bt \quad (2.10)$$

where  $a$  is the initial fluid temperature, which can be found from the temperature change vs. time in Figure 2, and  $b$  is the first derivative of temperature to time  $t$ , i.e.,  $b = dT_f/dt$ . Because  $t = Z/V$ ,  $V$  is constant, then

$$b = \left( \frac{dT_f}{dZ} \right) V \quad (2.11)$$

Similar to the above section, a heat balance on the pipe yields

$$C_v V \frac{dT}{dt} = -hA(T - T_f) = -hA(T - a - bt) \quad (2.12)$$

Let  $\theta = T - a$ , then one has

$$C_v V \frac{d\theta}{dt} = -hA(\theta - bt) \quad (2.13)$$

$$\theta_0 = T_0 - a \quad \text{at } t = 0$$

where  $T_0$  is the initial pipe temperature. The solution to equation (2.13) is

$$\theta = b \left( t - \frac{C_v L}{h} \right) + \left( \theta_0 + \left\{ \frac{C_v L}{h} b \right\} \right) e^{-\frac{h}{C_v L} t} \quad (2.14)$$

where  $L = V/A$ , is the characteristic length. Substitute  $\theta = T - a$  into the above equation, which yields the pipe temperature

$$T = T_f - b \left\{ \frac{C_v L}{h} \right\} + \left( T_0 - a + b \left\{ \frac{C_v L}{h} \right\} \right) e^{-\left\{ \frac{h}{C_v L} \right\} t} \quad (2.15)$$

The temperature difference of fluid and pipe is

$$T_f - T = b \left\{ \frac{C_v L}{h} \right\} + \left( a - T_0 - b \left\{ \frac{C_v L}{h} \right\} \right) e^{-\frac{h}{C_v L} t} \quad (2.16)$$

This temperature difference depends on the two terms in the right side of the equation. The first term is a constant dependent on pipe and fluid characteristics. The second term becomes smaller and smaller as time  $t$  increases. At initial time the temperature difference is  $(a - T_0)$ . As time increases, the second term becomes less

important gradually. Finally the temperature difference of fluid and pipe reaches a constant

$$(T_f - T)_{fin} = b \frac{C_v L}{h} \quad (2.17)$$

Substitute (2.11) into this equation, one has

$$(T_f - T)_{fin} = (V \frac{dT_f}{dZ}) (\frac{C_v L}{h}). \quad (2.18)$$

This shows the final temperature difference depends on the drill lowering speed, fluid temperature gradient, material characteristics, and the convective coefficient. Greater drill descent speed introduces greater temperature difference.

For a practical case, the calculated drill temperature while descending in the lower part of a borehole is shown with the dotted line in Figure 4. The data used are listed below:

- Drill descent speed:  $V = 0.53 \text{ m/s}$
- Volume heat capacity of drill:  $C_v = 3.67 \times 10^6 \text{ J/m}^3\text{C}$
- Pipe characteristic length:  $L = V/A = 1.27 \times 10^{-3} \text{ m}$
- Heat convective coefficient:  $h = 284 \text{ W/m}^2\text{C}$
- Fluid temperature profile used is shown in Figure 2

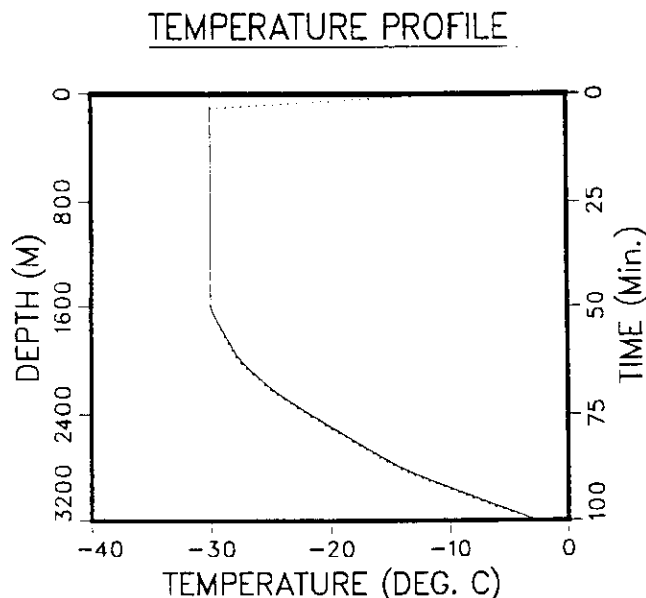


Figure 4. Sketch of ice drill temperature change with depth in the ice borehole filled with fluid. Dotted line - drill temperature; Solid line - fluid temperature. Descent speed is 0.53 m/s.

From Figure 4 one can see that the drill temperature changes from  $-10^{\circ}C$  to  $-30^{\circ}C$  during lowering from the surface to about a 64-m depth. Then the temperature remains constant (same as the fluid temperature) until a 1600-m depth. At this point the fluid temperature begins to change. As further depth is reached in the borehole, the drill has a temperature lag which gradually increases until the bottom is reached. The maximum lag is only about  $0.3^{\circ}C$ .

Formulas (2.16) and (2.18) can also be used to estimate the drill temperature change during drill retrieval in the borehole. Assume the drill has stayed on the borehole bottom for over two minutes. Then its temperature can be assumed the same as the surrounding fluid temperature. When lifting begins, the drill temperature becomes lower than the surrounding fluid temperature. This difference increases in the bottom 400 m of the borehole, but does not exceed  $0.3^{\circ}C$  for a lifting speed of 0.53 m/s. As lifting continues above the bottom 400-m zone, the temperature difference becomes smaller because the fluid temperature gradient decreases. When the drill is lifted into the upper 1600-m zone of the borehole, the drill temperature is the same as that of the fluid temperature.



## SECTION 3

### FREEZING OF MELT WATER

As shown in Figure 1, a standard drill used in the GISP-2 project is made of two stainless steel pipes. When going down to the bottom of a borehole, the melt water may freeze at the surfaces of both pipes and the borehole wall. This introduces an axisymmetric multiple-phase change problem which needs special treatment in the computer code for modeling. Here a 1-D finite element formulation for melt water freezing is described and followed by relative modeling results.

#### 3.1 Finite Element Formulation

The program developed here is capable of handling 1-D heat transfer problems in either Cartesian or radial coordinates. The following theory applies to both cases. The equation to be solved in each phase is the heat conduction equation

$$\bar{\nabla} (k \bar{\nabla} T) = C_v \frac{\partial}{\partial t} \quad (3.1)$$

with the phase interface boundary condition

$$L_v \frac{d\vec{S}}{dt} = (k \bar{\nabla} T)_f - (k \bar{\nabla} T)_u \quad (3.2)$$

Here

$T$  = temperature,

$t$  = time

$\vec{S}$  = location of the phase interface

$C_v$  = volumetric heat capacity

$L_v$  = volumetric latent heat

$k$  = thermal conductivity

The subscripts  $f$  and  $u$  refer to the frozen and unfrozen zones, respectively. The method of solution used the Dirac delta function to include the latent heat in the heat capacity in equation (3.1) to compute temperature distribution. Equation (3.2) was

used to specify the new locations of the phase lines at each time step. An implicit one-parameter "θ" scheme was used for the transient process. Using a weighted residual method (Galerkin method) with integration by parts on equation (3.1) together with boundary conditions, it is easy to get the general element matrix equations (Huebner and Thornton, 1982) as

$$[C] \left\{ \frac{dT}{dt} \right\} + ([K_c] + [K_h]) \{T\} = \{R_Q\} + \{R_q\} + \{R_h\} \quad (3.3)$$

where

$$\begin{aligned} [C] &= \int_{\Omega} C_v \{N\} \{N\} d\Omega \\ [K_c] &= \int_{\Omega} k \{B\}^T \{B\} d\Omega \\ [K_h] &= \int_{S_1} h \{N\} \{N\} dS \\ \{R_Q\} &= \int_{\Omega} Q \{N\} d\Omega \\ \{R_q\} &= \int_{S_2} q \{N\} d\Gamma \\ \{R_h\} &= \int_{S_1} h T \{N\} d\Gamma \end{aligned} \quad (3.4)$$

for Cartesian coordinates. For radial coordinates, simply add a variable  $r$ , radius, into the integrations in equations (3.4). For additional boundary conditions, e.g., radiation, just add more terms in equation (3.3). In equation (3.4),  $[C]$  is the capacitance (or mass) matrix,  $[K_c]$  and  $[K_h]$  are conductance matrixes related to conduction and convection, respectively. The convection matrix is computed only for elements with surface convection. The vectors  $\{R_Q\}$ ,  $\{R_q\}$  and  $\{R_h\}$  are for internal

heat generation, specified surface heating, and surface convection, respectively. The subscripts  $\Omega$  and  $s$  refer to the volume and surface area of integration respectively.  $N$  is the element shape function and  $B$  is the gradient function. For higher accuracy it is better to use the isoparametric element. For 1-D three-node element (Fig. 5) the shape function is

$$\begin{aligned}
 [N] &= [N_1, N_2, N_3] \\
 N_1 &= -\frac{1}{2}(1-\xi)\xi \\
 N_2 &= 1-\xi^2 \\
 N_3 &= \frac{1}{2}(1+\xi)\xi
 \end{aligned} \tag{3.5}$$

Then

$$X = [N] \{x_i\}$$

and

$$T = [N] \{T_i\}$$

where  $\{x_i\}$  and  $\{T_i\}$  are the node coordinates and temperatures respectively.

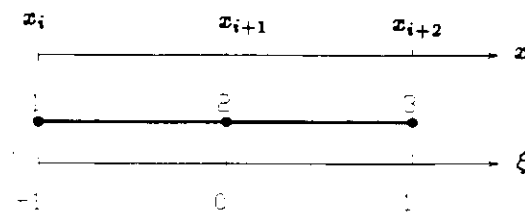


Figure 5. Three-node isoparametric element in  $\xi$  coordinate.

The gradient function

$$\begin{aligned}
 [B] &= [B_1, B_2, B_3] \\
 B_i &= \frac{\partial N_i}{\partial x} \quad i = 1, 2, 3
 \end{aligned} \tag{3.6}$$

Then

$$\frac{\partial T}{\partial x} = \left[ \frac{\partial N_i}{\partial x} \right] \{T\} = [B] \{T\}$$

For an element with phase change, the latent heat effects are accounted for through a Dirac delta function in the heat capacity. The Dirac delta function has properties

$$\delta(T - T_0) = \begin{cases} 0 & T \neq T_0 \\ \infty & T = T_0 \end{cases}$$

and

$$\int f(T) \delta(T - T_0) d\tau = f(T_0) \quad (3.7)$$

Let heat capacity

$$C_v = C_s + L\delta(T - T_0) \quad (3.8)$$

where

$C_s$  = sensible volume heat capacity

$L$  = volume latent heat

$T_0$  = freezing temperature

Thus, the element heat capacitance matrix for Cartesian coordinate may be written as

$$[C] = \int_x C_s \{N\} \{N\} dx + L \int_x \delta(T - T_0) \{N\} \{N\} dx. \quad (3.9)$$

The second term in equation (3.9) equates

$$L \int_x \delta(T - T_0) \{N\} \{N\} dx = L \{N\} \{N\}_{x=x_0} \quad (3.10)$$

where  $x_0$  is the phase line location. Thus,

$$[C] = \int_x C_s \{N\} \{N\} dx + L \{N\} \{N\}_{x=x_0} \quad (3.11)$$

For the radial coordinate

$$[C] = \int_r C_s \{N\} \{N\} r dr + L \{N\} \{N\}_{r=r_0} \quad (3.12)$$

where  $r_0$  is the phase line location. In this two-phase element the sensible heat capacity  $C_s$  and the thermal conductivity  $k$  were linearly averaged.

For the transient process, the basic implicit time scheme was as follows,

$$[K]\{T\}_{n+1} = \{\bar{R}\}_{n+1},$$

$$[\bar{K}] = \theta[K]\Delta t + [C],$$

$$[\bar{R}] = -(1 - \theta)[K]\Delta t + [C]\{T\}_n + ((1 - \theta)\{R\}_n + \theta\{R\}_{n+1})\Delta t \quad (3.13)$$

where  $\{R\}$  is the temperature load vector,  $\Delta t$  is the time step,  $\theta$  is a parameter, which may be chosen from 0 to 1, and 0.5 (Crank-Nicolson method) was used in the modeling.

### 3.2 Model Test

To test this finite element model, an analytical solution of a classical problem in phase change was chosen, which is often referred to as the Stefan problem. It can be illustrated as below in the water-ice system.

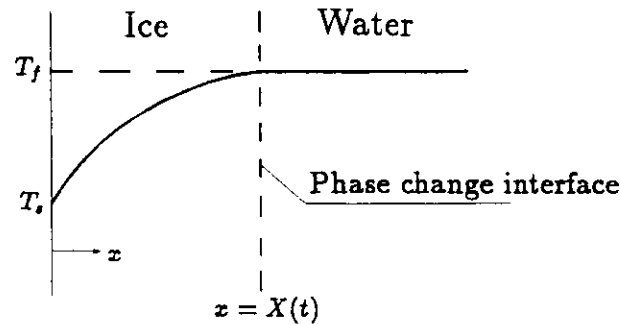


Figure 6. Temperature distribution in partially frozen water.

Initially, a semi-infinite region (water) is at a constant freezing temperature  $T_f$ , and the temperature of the surface is suddenly dropped to  $T_s$  and holds constant (step change at surface), as shown in Figure 6. The Stefan's solution of phase change location may be expressed as (Lunardini, 1981)

$$X(t) = \sqrt{\frac{2k_i(T_f - T_s)t}{L}} \quad (3.14)$$

where  $k_i$  is the ice thermal conductivity,  $t$  time, and  $L$  the volume latent heat. With  $k_i = 2.1 \text{ W/m}^\circ\text{C}$ ,  $L = 3 \times 10^8 \text{ J/m}^3$  and  $T_f - T_s = 10^\circ\text{C}$ , the calculated phase locations vs. time are shown with the solid line in Figure 7. To examine the finite element modeling with these results, a 3-node element was used with domain of 10-mm. Noticing that the Stefan's solution is subject to the assumption that  $\frac{C_i(T_f - T_s)}{2L}$  is small,  $C_i$  ice heat capacity, a value of  $C_i/10$  was used in the modeling test to be consistent with the Stefan's assumption. The modeling results are shown with the dashed line in Figure 7. Figure 7 shows that the finite element model can give satisfactory results for engineering needs in phase change problems.

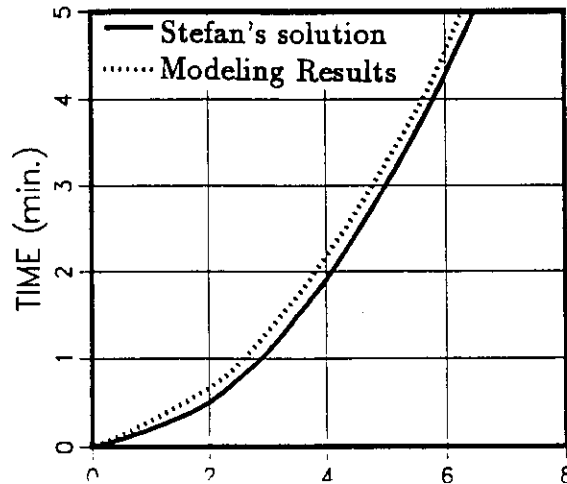


Figure 7. Water-ice phase locations vs. time. Solid line – Stefan's solution; Dashed line – Modeling results.  $T_f - T_s = 10^\circ\text{C}$ .

### 3.3 Standard Computation

As an example, the finite element model was run to compute the melt water freezing process around the drill in an ice borehole bottom in Greenland. First, the modeling domain is determined based on the drill sizes as shown in Figure 1. Because of the axisymmetry of the problem, the domain starts at the drill pipe axis as

the origin and extends in the radial direction to include the two drill pipe walls and into the borehole ice wall as shown in Figure 8.

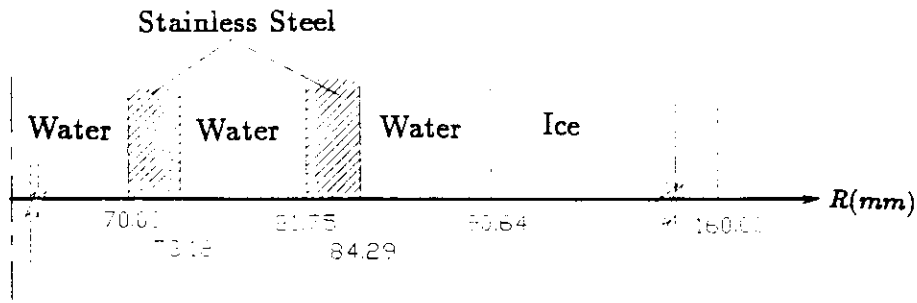


Figure 8. Standard modeling domain with 3-node 1-D element.

Second, the initial temperature of the modeling domain needs to be determined approximately. The initial drill temperature in the borehole is assumed to be the same as the ice wall temperature according to the analysis in the foregoing section. From the ice temperature profile shown in Figure 2, the temperature gradient is large in the bottom of the borehole. When the melt water goes up from the bottom, the temperature difference of melt water and the drill pipes as well as that of the ice wall increases gradually. The maximum difference depends on how high the melt water may reach in the borehole. For an extreme case a height of 25.5 m was accounted for in the modeling, which is the drill length. If the ice gradient in the bottom is constantly taken as  $5^{\circ}C/100m$  and the melt water temperature supposed at freezing point, the temperature of the ice wall is  $T_i = -2.4^{\circ}C - 25.5m \times 5^{\circ}C/100m \doteq -4^{\circ}$ . There are still some uncertainties in this estimation to the real situation. To be conservative, an ice temperature of  $-5^{\circ}C$  was used in the standard computation.

The temperature at the right boundary was set constant of  $-5^{\circ}C$ . Other relative parameters used in the modeling are listed in Table 1. The initial time step was 0.001s and changed to 1s after 1000 steps.

Table 1. Parameters and data used in the standard modeling.

	Melt Water	Stainless Steel	Ice
$C (J/mm^3^{\circ}C)$	$4.22 \times 10^{-3}$	$3.60 \times 10^{-3}$	$1.83 \times 10^{-3}$
$k (W/mm^{\circ}C)$	$0.56 \times 10^{-3}$	$16.30 \times 10^{-3}$	$2.10 \times 10^{-3}$
Initial Temp.	$-2.4^{\circ}C$	$-5^{\circ}C$	$-5^{\circ}C$

Freezing temperature =  $-2.4^{\circ}C$   
 Ice volume latent heat =  $300 \times 10^{-3} J/mm^3$

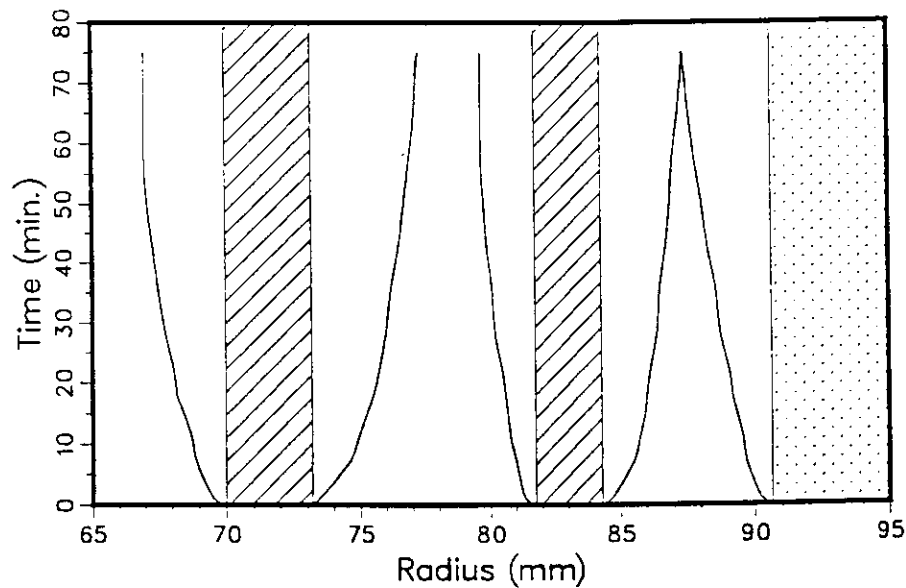


Figure 9. Melt water freezing time vs. the phase locations in radial direction. "Steel" – drill pipe walls; "Ice" – the ice borehole wall; "Water" – the meltwater. Initial temperature: Steel and Ice,  $-5^{\circ}C$ ; Water,  $-2.4^{\circ}C$ . Freezing temperature of melt water:  $-2.4^{\circ}C$

The modeling results of the melt water freezing process in the borehole are shown in Figure 9. In this particular case, there are five phase lines. One is in the inner drill pipe, and two within each space between the pipes and between the pipe and the ice wall. The two freezing fronts between the outer pipe and ice wall get closed first in about 75 minutes from beginning of freezing. The others are almost stable after 75 minutes, so there is no freezing-up (fronts close) in other spaces between the pipes and inside the inner pipe. The space between the outer pipe and



the ice wall is the control region for freezing of the drill into the bottom of a borehole by melt water.

Melt water freezing processes for ice temperatures of  $-10^{\circ}\text{C}$ ,  $-15^{\circ}\text{C}$  were also computed by the model. The freezing-up times in the control region between the outer pipe and ice wall are 24 minutes and 10.5 minutes respectively which can be found in Figure 10 for 0 percent of slush.

### 3.4 Freezing of Slush

In mechanical ice drilling, there are always ice chips produced in the borehole. If they are mixed into the melt water, the mixture of ice chips and melt water is called slush. Obviously the slush freezes more quickly than pure melt water under same temperature gradient due to the presence of ice chips. So the slush freezing in the borehole around the drill was also studied.

Similar to equation (3.2) the phase interface boundary condition for slush freezing can be written as

$$L_s \frac{d\bar{S}}{d} = (k\bar{\nabla}T)_f - (k\bar{\nabla}T)_u, \quad (3.15)$$

where  $L_s$  is the volume latent heat. This latent heat will be reduced due to the ice chips in the melt water at the phase change interface. If the volume fraction of ice chips in the mixture of melt water and ice chips is  $\alpha$ , then the volumetric latent heat of the slush is

$$L_s = (1 - \alpha)L \quad (3.16)$$

where  $L$  is the ice volume latent heat. The slush accelerates the rate of ice formation due to the reduced latent heat of the mixture of melt water and ice chips. All foregoing methods for computing the melt water freezing are valid if the formula (3.16) is used for latent heat.

In the computations of the slush freezing, different percentages (in volume) of ice chips in the mixture of melt water and ice chips were chosen, as 0%, 20%, 50% and 75%, with each at ice borehole wall temperatures of  $-5^{\circ}\text{C}$ ,  $-10^{\circ}\text{C}$  and  $-15^{\circ}\text{C}$ , respectively. The results of freezing-up time were then linearly regressed. These regression relations of freezing-up time versus volume percentage of ice chips in the slush are shown in Figure 10. The other drill parameters and dimensions used in the computations are the same as in the above section. From Figure 10, one can see the freezing-up time decreases quickly as the ice chip percentage increases in the melt water for ice temperature of  $-5^{\circ}\text{C}$ , but more slowly for a lower ice temperature, e.g.,  $-15^{\circ}\text{C}$ . For all ice temperatures the freezing-up time of slush with 75% ice chips is about 0.44 times the freezing-up time for pure melt water.

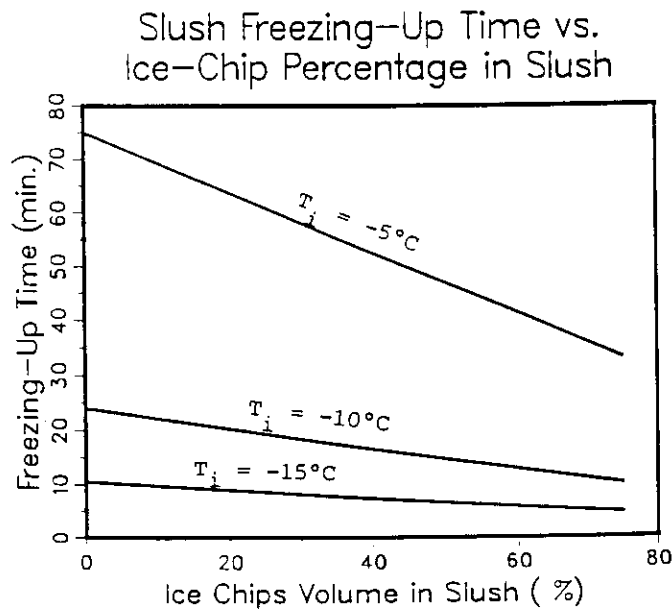


Figure 10. Freezing-up (phase fronts close up) time of slush (mixture of meltwater and ice chips) vs. volume percentage of ice chips in the slush.  $T_i$  is the ice borehole wall temperature.

## SECTION 4

### CONCLUSIONS AND SUGGESTIONS

To estimate possible drill freezing into the borehole by melt water, the drill temperature change during descent in the borehole was analyzed. For a drill used in the GISP-2 project, it will take two minutes to change the drill temperature by 20°C. So the drill temperature can be assumed to be the same as that of the surrounding liquid filled in the upper borehole where the ice temperature is nearly constant in the vertical direction. When lowering to the bottom of an iceborehole, the drill temperature increases gradually as the filled liquid temperature increases, but with a lag in the liquid temperature. This lag depends on the drill lowering speed and the vertical ice temperature gradient. For a descent speed of 0.53 m/s, this lag is less than 0.3°C, a very small value.

For drill freezing into the bottom of a borehole by melt water, the control zone is the space between the outer drill pipe and the ice wall where freezing fronts from the pipe surface and the ice wall close first. Due to the temperatures of ice and drill at the bottom being relatively warm (-5°C assumed), this freezing-up process takes about 75 minutes for pure melt water. While for slush, mixture of ice chips and melt water, the freezing accelerates. For 75% volume of ice chips in the slush, the freezing-up time decreases to 0.44 times of that for the pure melt water.

To reduce the possibility of the drill freezing into the bottom of a borehole by the melt water, some practical measures may be taken account for. One is using an appropriate drill descent speed, especially lowering slowly in the bottom region of the borehole. This gives the drill more time to uniform its temperature distribution to close to the surrounding melt water temperature, and therefore the freezing rate can be reduced. Another method to reduce the freezing rate is to decrease the freezing temperature. This can be achieved by moving the drill up and down several times when it reaches the bottom of a borehole. By moving the drill, the melt water can be

mixed with the filled liquid which has a freezing temperature far lower than melt water. Therefore, the freezing temperature of the melt water mixed with the liquid is decreased. Even if the freezing begins at the drill surface, the fresh ice is very weak when near the freezing temperature, and may be easily broken by the moving drill.

## REFERENCES

- Eckert, E. R. G. and R. M. Drake, Jr. 1972. *Analysis of Heat and Mass Transfer*. McGraw-Hill Book Company. p 806.
- Huebner, K. H. and E. A. Thornton. 1982. *The Finite Element Method for Engineers*. John Wiley & Sons. p 623.
- Kay, J. M. 1963. *An Introduction to Fluid Mechanics and Heat Transfer*. 2nd Edition. Cambridge Press. p 327.
- Lunardini, V. J. 1981. *Heat Transfer in Cold Climates*. Van Nostrand Reinhold Company. p 731.
- O'Neill, K. 1983. "Solution of 2-D Axisymmetric Phase Change Problems on a Fixed Mesh, with Zero Width Phase Change Zone," *Numerical Methods in Thermal Problems*. In R. W. Lewis, J. A. Johnson and W. R. Smith (eds.) Proceedings of the 3rd International Conference. p 134-146.
- Spring, U. 1981. "Reply to: A Comment on 'Pressure Melting,'" *Cold Regions Science and Technology* 4:157.